have an average value of 1) is obtained by a computer simulation of Brownian molecules, and RD values that give 2.5 (or 5; these are typical values and could be adjusted for the individual studies) percentile of the molecules from both ends of the distribution, referred to as RD_{min} and RD_{max}, are determined (Figure 19.7). When the trajectory of an experimental molecule shows an RD value between RD_{min} and RD_{max}, it is classified into the simple Brownian diffusion mode, and when $RD > RD_{max}$ or $RD < RD_{min}$, it is classified into the directed or confined/hop diffusion mode, respectively.

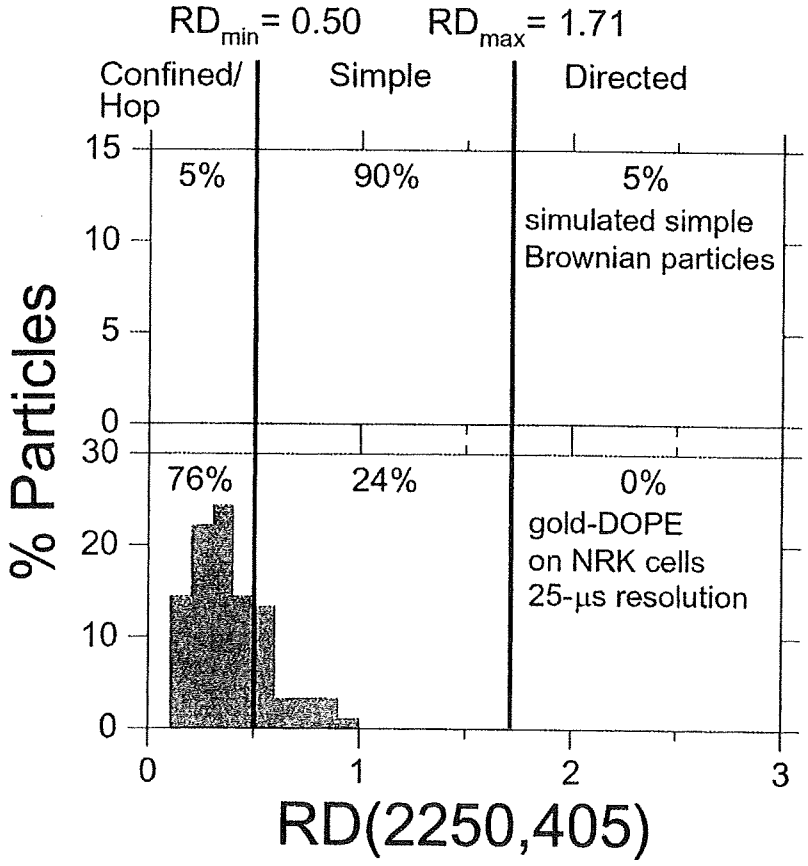

Figure 19.7 The distribution of RD for gold-tagged DOPE molecules observed in the plasma membrane of NRK cells at a 25-μs resolution (*bottom*) is quite different from that expected from simulated simple Brownian particles (*top*). In this example, the total number of frames in each trajectory is 2250 steps (56 ms) and the analysis window (Δt) is 405 steps (10 ms). For the classification of the trajectories into the three modes of motion, 1 000 simple Brownian trajectories were generated by Monte Carlo simulations, and the RD values that give 5% of the particles from both ends of the distribution were determined (RD_{min} of 0.50 and RD_{max} of 1.71, shown by bold vertical lines). When an experimental trajectory exhibited an RD value smaller than RD_{min} or greater than RD_{max}, it was classified into the confined/hop or directed diffusion mode, respectively. The majority (76%) of the DOPE trajectories ($N = 90$) were classified into the confined/hop mode at a time resolution of 25 μs.

This is a simplified, but practical approach to anomalous diffusion discussed throughout this book, although there may be finer or more elegant ways of describing anomalous diffusion (see the Chapters by Kimmich et al., Shlesinger, and Chechkin et al. in this book). Furthermore, the diffusion data have to be analyzed and interpreted, based on or in the way consistent with the data on the membrane-associated part of the actin cytoskeleton meshwork observed by electron tomography with subnanometer precisions [35] as well as single-molecule force measurements on membrane molecules [49, 51, 72]. Interpretations simply based on the analysis of the diffusion measurements, particularly done at low-time resolutions or for a collection of molecules, have to be re-examined based on these other important observations.

Therefore, the goal of analyzing results obtained by single-molecule tracking in the plasma membrane is to classify each experimental trajectory into one of these motional modes and to obtain the distribution or the histogram of the parameters characterizing each motional mode. Fitting the above theoretical $MSD(\Delta t) - \Delta t$ equation to the experimental $MSD(\Delta t) - \Delta t$ plot, independently in two orthogonal directions, quantitatively provides estimates for various diffusion parameters. Furthermore, for hop diffusion, individual compartments in each trajectory can be detected automatically by a computer program (see the methods section of Suzuki et al. [67] for details). Briefly, a variable size window in time is moved through the trajectory, and the local diffusivity is recorded. Intercompartmental jumps are seen as sharp increases in the diffusivity of the molecule as it extends its motion into a neighboring compartment.

The hop rates of transferrin receptor for the smaller and greater compartments in NRK cells (NRK cells have a plasma membrane with nested double compartments with sizes of 230 and 710 nm, Fujiwara et al. [12]) were recently found to be an average of every 55 and 570 ms (direct SPT measurements gave 55 and 1800 ms, respectively, but the latter value needed to be corrected for the crosslinking effect of gold probes, using a macroscopic diffusion coefficient determined by SFMT with fluorescently labeled transferrin (a time window of 3 s, giving 0.22 $\mu m^2/s$) and the compartment size determined by SPT (710 nm)) [12]. Furthermore, all of the transmembrane proteins examined thus far, including E-cadherin [51], transferrin receptor [48], α2-macroglobulin receptor [48], CD44 (Ritchie and Kusumi, unpublished observations), band 3 [72], stem cell factor receptor (Kobayashi, Murakami, and Kusumi, unpublished observations), and various GPCRs (Suzuki et al. [67], Kasai, Prossnitz, and Kusumi, unpublished observations), undergo hop diffusion. The macroscopic diffusion coefficients for these molecules, determined by SPT (reflecting hop diffusion rate over many compartments), are basically consistent with the SFMT and FRAP data, although due to the crosslinking effects of gold probes, the macroscopic diffusion coefficients may be smaller by a factor of 1–5. Since,

even in the presence of crosslinking effects, the compartment sizes determined by SPT are likely to be correct, a good strategy to evaluate the correct average hop frequency across the compartment boundaries (inverse the average residency time within a compartment) is to use the macroscopic diffusion coefficient determined by SFMT with fluorescent probes and the compartment size obtained by SPT, using the equation,

$$\text{Residency time} = \frac{(\text{Average compartment size from SPT})^2}{(4 \times D_{\text{MACRO}} \text{ from SFMT})}. \tag{19.5}$$

With this equation, one assumes a stylized model of hop diffusion (for the purpose of simple calculation), in which the molecule undergoes diffusion in the presence of an equally spaced, infinite array of barriers of the same height, and the hops occur between the central points in the compartments. Murase et al. [37] successfully employed this strategy to obtain the residency time as well as the permeability of the barriers in the plasma membranes for a phospholipid molecule, in a variety of cultured mammalian cells.

19.5 Corralling Effects of the Membrane Skeleton for Transmembrane Proteins (the Membrane-Skeleton Fence Model)

What makes the boundaries between these compartments for transmembrane proteins? We proposed the "membrane-skeleton fence" or "membrane-skeleton corralling" model (Figure 19.8, left). Transmembrane proteins protrude into the cytoplasm, and, in this model, their cytoplasmic domains collide with the membrane skeleton, which induces temporary confinement

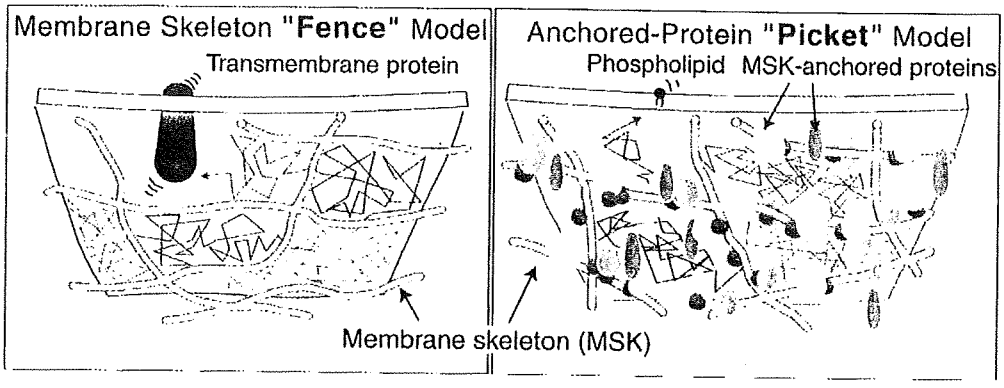

Figure 19.8 The effects of the membrane-skeleton "fence" (left) and the anchored-protein "pickets" (right) that together partition the entire plasma membrane into small compartments. See the text for further details. The hydrodynamic-friction-like effect was first described by Bussell et al. [2, 3].

or corralling of the transmembrane proteins in the membrane skeleton mesh. Transmembrane proteins may hop between the compartments when a space that allows the passage of the cytoplasmic domain of the transmembrane protein is formed between the membrane and the membrane skeleton. This space may be created as a consequence of the thermal fluctuation of these structures, when the actin filament that forms the compartment boundary temporarily dissociates, and/or when the transmembrane protein incidentally has sufficient kinetic energy to overcome the confining potential energy of the compartment barrier when it is in the boundary region.

Here is a summary for the evidence supporting the membrane skeleton fence model for the partitioning of the cell membrane with respect to transmembrane proteins. The problems with other models, including raft-induced compartmentalization of the plasma membrane, crowding of the extracellular surface by the extracellular domains of membrane molecules, protrusions and dips throughout the membrane, and/or a two-dimensional continuum fluid, are that they can explain one or several of these observations, but not *all* of these observations.

(1) The hop rate of band 3 in the red-cell ghost membrane and that for E-cadherin in cultured L cells (both are transmembrane proteins) were increased with a decrease in the cytoplasmic domain size [51, 72]. This clearly indicates that the cytoplasmic domain of the transmembrane protein is involved in temporarily trapping the transmembrane protein.

(2) When each individual transmembrane protein molecule was dragged by an optical trap (transferrin receptor and E-cadherin), the compartment size estimated by the free dragging length in optical trap experiments employing very weak trapping forces agrees with that detected by single-molecule diffusion measurements [49, 51], indicating the presence of actual force barriers between the compartments.

(3) The experiments in which each individual molecule of transferrin receptor, E-cadherin, and band 3 was dragged using an optical trap revealed that the compartment boundaries are elastic, consistent with the model in which the basis for the compartment barrier is the membrane skeleton meshwork [49, 51, 72].

(4) When the membrane skeleton is dragged, by moving the optical trap that grabbed a polystyrene bead bound to the membrane skeleton, transmembrane proteins (band 3) that are not bound to the membrane skeleton and undergo diffusion were also moved, along with the movement of the membrane skeleton [72].

(5) Hop diffusion of transmembrane proteins depends on the integrity of the membrane skeleton [48, 67, 72]. Very mild latrunculin or cytochalasin D treatments increased the average compartment size. Note that since harsher treatments tend to induce membrane protein aggregation and overall changes in the cell shape, making the interpretation of diffusion data virtually impossible, only very mild treatments are useful. Under these conditions, one should note that the effects of these drugs are complex, depending on the treatment duration (because cells start compensating for the initial changes in the actin filaments), the cell type (the overall amounts of actin and the ratio of the amounts of actin molecules in stress fibers vs. single filaments), the action mechanisms of the drugs, and the drug concentrations. Furthermore, the effects of latrunculin or cytochalasin D are difficult to find if one measures the macroscopic diffusion coefficients by FRAP or slow-rate (like video-rate) single-molecule tracking, because, after cells are treated with these drugs, the compartment size slightly increases, whereas the hop rate tends to decrease slightly, resulting in only minor increases in the macroscopic diffusion coefficient (between a factor of 1 and 2). In fact, several reports have noted the absence of the effects of latrunculin, cytochalasin, gelsolin, and siRNA of spectrin on the movement of various membrane molecules [11, 32, 41, 58, 77], whereas Lenne et al. [30], using fluorescence correlation spectroscopy, found that the diffusion of transferrin receptor is affected by drugs that target the actin-based membrane skeleton.

Furthermore, hop diffusion could not be found in liposomes and in membrane blebs, where the membrane skeleton is essentially absent (Suzuki et al. [67]; in some cell types, considerable fractions of the actin skeleton remain in the blebbed membrane, and if this happens, the membrane has to be further treated with latrunculin or cytochalasin D to remove the remaining actin skeleton, for the elimination of hop diffusion). In these membranes, the membrane molecules undergo rapid, simple Brownian diffusion that can be characterized by a single diffusion coefficient in the range of 5–10 $\mu m^2/s$ for DOPE or 3 $\mu m^2/s$ for transmembrane proteins in all of the observation time scales (0.025 ms–1 s, i.e., by a factor of 40 000).

(6) Electron microscopy results, in particular those with rapidly frozen, deeply etched specimens of the plasma membranes [35] or those obtained with a scanning electron microscope (Morone and Kusumi, unpublished observations), showed that, except for the specific locations where internalization apparati, cell adhesion structures, microvilli, or filopodia are located, the plasma membrane exhibits a gently undulating surface, which generally lacks sharp protrusions or dips. In fact, in our previous observations of high-speed single-particle tracking, the candidate

cell lines were first examined by scanning electron microscopy, and only those without too many microvilli were selected for our observations. The presence of membrane protrusions and dips has been thought to cause apparent confinement. However, this cannot be true. First, to reduce the macroscopic diffusion coefficient by a factor of 10, the protrusions or dips must be as large as 100–300 nm for a compartment size of 200 nm, and they must be present throughout the cell membrane. This is clearly inconsistent with the electron microscope observations (possibly except for the brush-border membranes of epithelial cells) [35,46]. Furthermore, the idea of membrane protrusions and/or dips for the apparent confinement is inconsistent with the observations (1), (2), and (3) described above.

(7) The instances of hops are clearly visible and also are detectable with a computer program in the analysis of single-molecule trajectories with sufficient time resolutions [67].

(8) Oligomerization of transmembrane proteins reduces the macroscopic diffusion coefficient by decreasing the intercompartmental hop rate (without affecting the compartment size), a phenomenon termed oligomerization-induced trapping by [18]. This can be easily explained by the membrane skeleton fence model, but cannot be naturally explained by the two-dimensional continuum fluid model, the viscoelastic model, the general anomalous diffusion model, or the model of long membrane protrusions and deep dips throughout the membrane.

The other aspect of this result is that it indicates a need for control experiments for the crosslinking effect of the gold probes using SFMT or FRAP, when SPT with gold particles is employed. To circumvent such a nuisance, in our lab, we always begin our studies using SFMT with a fluorescent tag, and only when we need high-speed single molecule tracking or when we wish to carry out optical trapping experiments, we develop colloidal gold probes. The crosslinking effect could become very extensive, so that it could cause the long-term trapping of the target protein within a compartment, when the probes were attached to cells at lower temperatures for over several 10s of minutes [4,5,67].

19.6 Phospholipids Also Undergo Hop Diffusion in the Plasma Membrane

The next natural question is "What about lipids?" Fujiwara et al. [12] and Murase et al. [37] indeed addressed this question, by observing an unsaturated phospholipid, L-α-dioleoylphosphatidylethanolamine (DOPE), which is considered to be one of the most difficult molecules to immobilize in the

plasma membrane, due to its unsaturation and low-levels of headgroup interactions. To observe the movement of single DOPE molecules, the DOPE was tagged with the fluorescent dye Cy3 or with a 40-nm diameter colloidal gold particle, and was observed by SFMT and SPT, respectively. The colloidal gold probes were necessary to observe DOPE diffusion at frame rates much higher than video rate (30 Hz). Due to low sensitivity, SFMT would not accommodate observations at frame rates much faster than 200 Hz. In video-rate observations (30 Hz) and in NRK cells, both methods yielded about the same diffusion coefficients, as long as they remained in time windows shorter than 100 ms. This result justifies the use of such a large colloidal gold particle as a probe for a small molecule, like DOPE. In longer time scales, the diffusion coefficient of gold-tagged DOPE was smaller than that of Cy3-tagged DOPE by a factor of 3, due to the crosslinking effect of gold probes (Fujiwara et al. [12], which, by the way, in itself shows that the plasma membrane cannot be considered as a two-dimensional continuum fluid).

Using high-speed SPT with a time resolution of 25 μs (a frame rate of 40 kHz, about 1300-fold faster than normal video rate), Fujiwara et al. [12] and Murase et al. [37] found that an unsaturated phospholipid, DOPE, undergoes hop diffusion. Representative trajectories of DOPE in the plasma membrane of NRK cells, recorded at time resolutions of 33 ms and 25 μs, are shown in Figure 19.9. At a 33-ms resolution (normal video rate), practically all of the DOPE trajectories were classified into the simple Brownian diffusion mode. However, when the time resolution was enhanced to 25 μs, it became clear that the simple Brownian nature found at the 33-ms resolution is only an apparent one. The hop diffusion is clearly visible (individual compartments were detected by the computer program we developed), and the statistical analysis method described above indeed showed that over 85% of the DOPE trajectories were classified into the hop-confined diffusion mode, rather than the simple Brownian diffusion mode.

Quantitative analysis of the trajectories, such as those displayed in Figure 19.6, revealed that the average compartment size was 230 nm in the case of NRK cells. The average residency time within each 230-nm compartment was 11 ms. No wonder we did not see hop movement at video rate, with a time resolution of only 33 ms. In fact, all of these trajectories shown in Figure 19.9 (bottom) are 62-milliseconds long, and if we had used video rate observations, there would have been only 2 or 3 points in the whole trajectory, and there would have been no way of detecting the hop diffusion of DOPE molecules. The diffusion rate within the 230-nm compartment, which is 5.4 $\mu m^2/s$ on average, is interesting. It is almost as large as that of DOPE molecules observed in artificial membranes, such as giant liposomes. Therefore, lipid diffusion in the cell membrane is slow, not because the diffusion per se is slow,

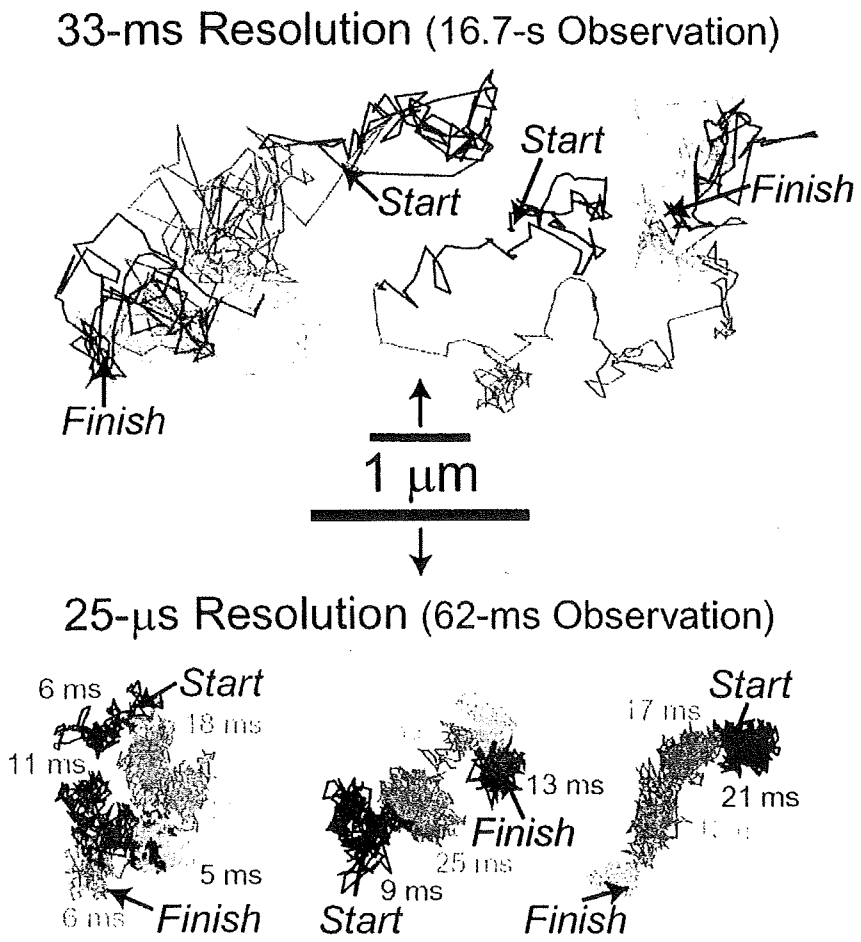

Figure 19.9 Representative trajectories of single or small groups of DOPE molecules recorded at time resolutions of 33 ms and 25 μs (see the text for details). The different colors of the trajectories obtained at a 33-ms resolution simply represent a time sequence of every 3.3 s. The different colors in the bottom trajectories obtained at a 25-μs resolution represent various plausible compartments, detected by computer software developed in our laboratory (in a time sequence of purple, blue, green, orange, and red for both time resolutions). These results show that the simple Brownian nature of diffusion observed at a video rate (33 ms/frame) is only superficial, and that it is due to the low-time resolution of the observation: the confined + hop movement of each DOPE molecule is totally smeared out at video rate. To resolve such movement, the time resolution must be considerably shorter than the average residency time within a compartment.

but because (1) the plasma membrane is compartmentalized with regard to the translational diffusion of phospholipids, (2) the lipid molecules undergo hop diffusion over these compartments, and (3) it takes time to hop from a compartment to an adjacent one (Figure 19.3). These observations solved the 30-year old enigma in the fluid mosaic model: the mechanism underlying the reduction of the diffusion rate in the plasma membrane by a factor of $\sim$ 20 from that found in artificial membranes.

What makes the boundaries between these compartments, which even work for phospholipids located in the outer leaflet of the membrane? Fujiwara et al. [12] observed DOPE diffusion in membrane blebs (balloon-like structures of the plasma membranes, where the membrane skeleton is largely lost, and Fujiwara et al. further reduced the actin-based membrane skeleton by treating the cells with latrunculin) as well as in liposomes, and found that DOPE molecules undergo rapid, simple Brownian diffusion with a diffusion coefficient of $\approx 9\ \mu m^2/s$ in these membranes. Furthermore, Fujiwara et al. [12] and Murase et al. [37] examined the involvement of the membrane skeleton, as well as the effects of the extracellular matrices, the extracellular domains of membrane proteins, and the cholesterol-rich raft domains, in phospholipid hop diffusion. They found that the phospholipid movement was only affected when they modulated the membrane skeleton with actin drugs. This is consistent with the previous FRAP observations, in the sense that the modulation of the membrane skeleton influences the lipid movement (although FRAP did not allow researchers to observe such detailed motion; see Paller [42]). All of these results point to the involvement of the membrane skeleton in both the temporal corralling and hop diffusion of phospholipids.

However, this is a very strange and surprising result! Since the DOPE molecules they observed were located in the extracellular leaflet of the membrane (unlabeled DOPE may flip, but the large DOPE molecule tagged with a gold particle cannot flip to enter the cytoplasmic leaflet), whereas the membrane skeleton is located on the cytoplasmic surface of the membrane, the DOPE and the membrane skeleton cannot interact directly. To explain this apparent discrepancy, the "anchored transmembrane-protein picket model" was proposed (Figure 19.8, right). In this model, various transmembrane proteins anchored to and lined up along the membrane skeleton (fence) effectively act as rows of pickets (these transmembrane proteins act like posts for the fence, and are thus termed pickets) against the free diffusion of phospholipids, due to steric hindrance as well as the hydrodynamic-friction-like effects of immobilized anchored membrane protein pickets. The latter effect, first proposed by Hammer's group [2, 3], propagates over about several nanometers, and is prominent in the membrane because the membrane viscosity is much greater than that of water, by a factor of $\approx$ 100, and is particularly marked when immobile pickets are aligned along the membrane-skeleton fence. When the number density of these transmembrane picket proteins exceeds a certain threshold (20–30% coverage of the intercompartmental boundary to reproduce the experimentally observed residency time of 11 ms in a 230-nm compartment in NRK cells, as determined by a series of Monte Carlo simulations by Fujiwara et al. [12]), the rows of pickets on the membrane-skeleton fences become effective diffusion barriers that confine the phospholipids for some time. Note that these transmembrane picket proteins do not have to be stably

bound to the membrane skeleton for a long time. Assuming that the boundary region between the compartments is 10 nm wide, it takes about 10 μs for a molecule to traverse this region. Therefore, the zeroth approximation is that if a transmembrane protein is bound to the membrane skeleton for at least 10 μs, then it becomes an effective picket to participate in the formation of the diffusion barrier. Note that, in this model, the transmembrane proteins anchored to the membrane skeleton are coupling the membrane skeleton, which is located on the cytoplasmic surface of the membrane, with the phospholipids that are located in the outer leaflet of the membrane.

Here, the evidence supporting the anchored-protein picket model (and membrane-skeleton fence model) is summarized.

(1) As described in point 5 for the membrane-skeleton fence model, the hop diffusion of DOPE depends on the integrity of the membrane skeleton [12, 37, 39]. Similar cautionary remarks can be applied to DOPE diffusion. Furthermore, hop diffusion cannot be found in liposomes and in membrane blebs, where the membrane skeleton is largely absent [12]. In these membranes, the membrane molecules undergo rapid, simple Brownian diffusion that can be characterized by a single diffusion coefficient, in the range of 5–10 $\mu m^2/s$ for DOPE, in all of the observation time scales (0.025 ms–1 s, i.e., by a factor of 40 000).

(2) Using electron tomography of rapidly frozen, deeply etched specimens of plasma membranes, Morone et al. [35] determined the distribution of the mesh size of the actin-based membrane skeleton right on the cytoplasmic surface of the plasma membrane, and found that it agrees well with that for the compartment size determined from the DOPE diffusion data (Figure 19.10). Good agreements between the electron tomography data and the DOPE diffusion results were observed for two cell types, NRK and FRSK cells, which exhibited quite different compartment sizes for DOPE diffusion, 230 nm and 42 nm, respectively, further supporting the anchored-protein picket model. In addition, their results showed that the cytoplasmic surface of the entire plasma membrane is coated with the actin-based membrane skeleton, except for the locations of the internalization apparati and cell adhesion structures.

(3) In the case of the human erythrocyte ghost, the compartment size determined from the diffusion measurements of transmembrane proteins and lipids is consistent with the mesh size of the spectrin-based membrane skeleton on the cytoplasmic surface of the ghost membrane, determined by AFM [70, 72].

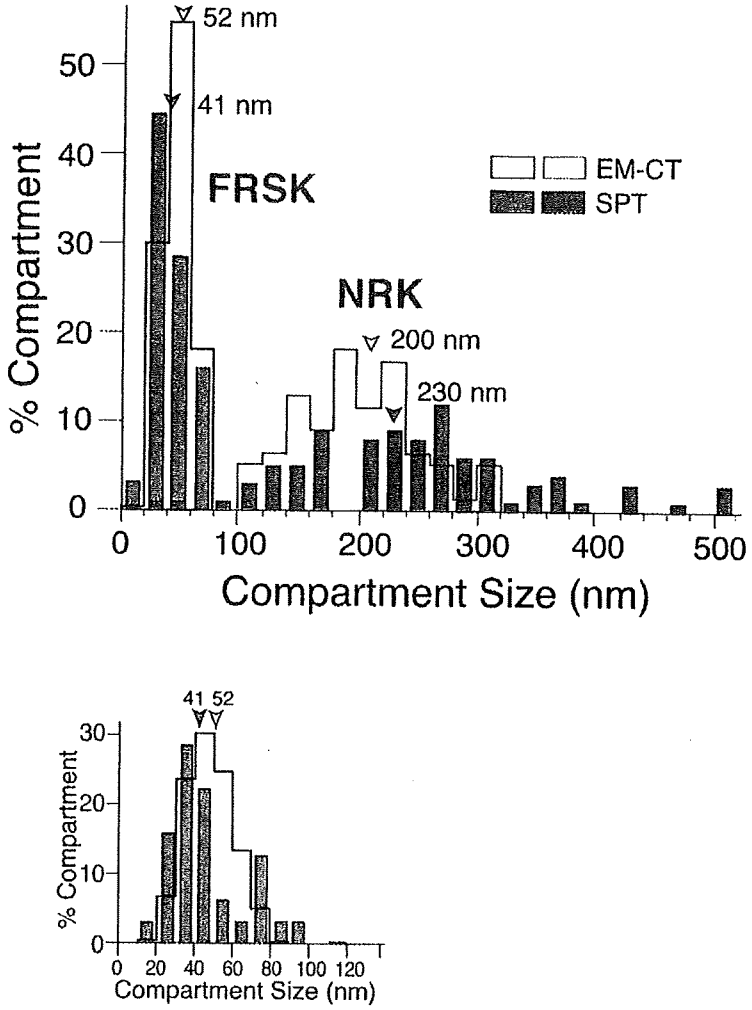

Figure 19.10 Comparison of the distributions of the membrane-skeleton mesh size on the cytoplasmic surface of the plasma membrane estimated by electron tomography (open bars), with that of the compartment size determined from the phospholipid diffusion data (closed bars, adapted from Fujiwara et al. [12] and Murase et al. [37]), for NRK (magenta) and FRSK (blue) cells. Within the same cell type, the MSK mesh size and the diffusion compartment size exhibited similar distributions (compare the open and closed bars with the same color). The actual sizes are quite different between NRK and FRSK cells. The bottom figure shows the histograms for FRSK in more detail.

(4) Mild treatments with jasplakinolide, which stabilizes the actin filaments, reduced the macroscopic diffusion coefficient, without strongly affecting the compartment size, by decreasing the hop frequency [12,37,39].

(5) As mentioned in point 8 for the membrane-skeleton fence model (oligomerization-induced trapping found for E-cadherin), the oligomerization of DOPE by crosslinking gold probes considerably reduced the inter-

compartmental hop rate, without affecting the compartment size, which thus decreased the macroscopic diffusion coefficient [37]. This entails the oligomerization-induced trapping of a phospholipid. This dependence of the diffusion coefficient on the diffusant size can easily be explained by the anchored-protein picket model, due to the steric effects, but not by other models.

(6) The hop diffusion is not affected by removing the major fraction of the extracellular domains of transmembrane proteins and the extracellular matrix [12,37], indicating that these are not the major causes for the induction of hop diffusion.

(7) The removal of cholesterol has no major effects on the hop diffusion [12, 37], suggesting that lipid rafts are not the primary causes for membrane compartmentalization or hop diffusion.

(8) The compartment sizes detected by transmembrane proteins (transferrin receptor, α_2-macroglobulin receptor) and the phospholipid DOPE are the same in all of the cell types examined thus far ([12, 48], Fujiwara, Iwasawa, and Kusumi, unpublished observations, Murase and Kusumi, unpublished observations), supporting the membrane-skeleton fence and anchored-protein picket models.

(9) Monte Carlo simulations reproduced the experimentally observed residency times when only 20–30% of the compartment boundaries were occupied by the anchored transmembrane protein pickets [12, 37, 39]. This represents the anchoring of only about 15% of the total transmembrane proteins in the plasma membrane.

(10) The instances of hops are clearly visible and also are detectable with a computer program in the analysis of single-molecule observations with sufficient time resolution [12, 37].

The anchored transmembrane protein pickets would be operative on any molecules incorporated in the membrane, including transmembrane proteins. Therefore, the diffusion of transmembrane proteins will be doubly suppressed in the membrane. Both the fence and picket will act on transmembrane proteins.

The oligomerization-induced trapping described above in point (5) indicates that the intercompartmental hop rate, or the residency time within a compartment, strongly depends on the oligomer size. Therefore, the correct residency time for monomeric DOPE (or other molecules) within a compartment was estimated, using the macroscopic diffusion coefficient obtained from single fluorescent-molecule tracking (SFMT) at a video rate and the compartment size obtained from the high-speed SPT (this should not be affected

by oligomerization) with the use of the equation [compartment size]^2/4D. In the slow frame-rate regime, the diffusing molecule can be modeled as that hopping between the centers of adjacent compartments. This was necessary because, with single fluorophore observations, obtaining trajectories with both a sufficient length and time resolution is difficult, due to poor signal-to-noise ratios and photobleaching.

How universal is this plasma membrane compartmentalization? Using the unsaturated phospholipid DOPE, Murase et al. [37] found such plasma membrane compartmentalization in all of the nine mammalian cells they examined. This list has slightly expanded since then, and in the 11 types of cultured mammalian cells we have analyzed, we detected the hop diffusion of DOPE incorporated in the plasma membrane. Among the different cell types, the compartment size varies greatly, from 30 nm up to 230 nm, and the residency time of DOPE varies between 1 and 17 ms.

Several recent studies reported the failure to detect such hop diffusion, but the experimental methods employed in these studies appear to be suboptimal, with unsuitable spatial resolutions, low frame rates, short overall observation durations for a single molecule, and wrong time scales for tracking etc [30, 78, 79].

19.7 The Biological Significance of Oligomerization-Induced Trapping Based on the Membrane-Skeleton Fences and Pickets

In the earlier part of this review, it was stated that one of the two long-standing problems for biophysicists studying molecular diffusion in the plasma membrane is that we do not understand why the macroscopic diffusion coefficients considerably decrease when membrane molecules, including receptor molecules and other signaling molecules in the membrane, form oligomers or molecular complexes [17, 18, 40]. These observations are completely opposite from the general view of membrane biophysicists. The theory by Saffman and Delbrück (1975) and experiments by Peters and Cherry [43] and Vaz et al. [75] consistently showed that translational diffusion is very *insensitive* to the diffusant size.

The partitioning of the plasma membrane into many small compartments could explain why the diffusion in the plasma membrane is very sensitive to oligomerization or the formation of molecular complexes (Figure 19.11, left), in contrast to the prediction from the two-dimensional continuum fluid model (Figure 19.11, right). These points have been already touched upon as evidence to support the fence and picket models, but they are more comprehensively described here. Monomers of membrane molecules may hop across the

picket-fence with relative ease, but upon oligomerization or molecular complex formation, the oligomers or the complexes as a whole, rather than single molecules, have to hop across the picket-fence all at once, and therefore, much more free space that lasts longer is required for the passage of these oligomers across the picket-fence of the intercompartmental boundary. Hence, these complexes are likely to have a much slower rate of hopping between the compartments, as found with oligomers of DOPE [37]. In addition, molecular complexes are more likely to be bound or tethered to the membrane skeleton, perhaps temporarily, which also induces (temporary) immobilization or trapping of molecular complexes. Such enhanced confinement and binding effects induced by oligomerization or molecular complex formation were collectively termed *"oligomerization-induced trapping"* [18,24].

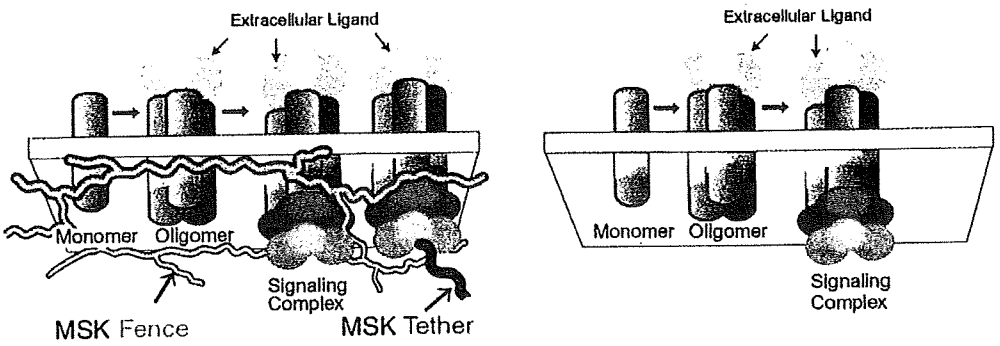

Figure 19.11 Oligomerization-induced trapping model, indicating how slowing or immobilization of membrane molecules may be induced upon oligomerization or the formation of greater molecular complexes. Upon oligomerization or molecular complex formation (left), the hop rate across the intercompartmental barrier would be reduced greatly, because, in contrast to monomers, in the case of molecular complexes, all of the molecules that form the complex have to hop across the picket-fence simultaneously, which requires greater and longer openings in the intercompartmental boundaries. In addition, due to the avidity effect, molecular complexes are more likely to be tethered to the membrane skeleton, perhaps temporarily, which also reduces their overall diffusion rate. This enhanced confinement and the binding effects induced by oligomerization or molecular complex formation are collectively termed "oligomerization-induced trapping" [18]. This would not occur in the absence of membrane skeleton fences and pickets (right).

This oligomerization-induced trapping might play very important roles in the temporary localization of signal transduction complexes (Figure 19.11, left). When an extracellular signal is received by a receptor molecule, the receptor often forms oligomers and signaling complexes by recruiting cytoplasmic signaling molecules. Due to the "oligomerization-induced trapping", these oligomeric complexes tend to be trapped in the same membrane skeleton compartment as that where the extracellular signal was initially received. Therefore, the membrane skeleton fence and the anchored transmembrane-protein pickets help to temporarily localize the initiation of the cytoplasmic signal to the place where the extracellular signal was received. Such spatial

confinement is particularly important for signals that induce local or polarized reorganization of the cytoskeleton or chemotactic events.

This would not occur in the absence of membrane skeleton fences and pickets (Figure 19.11). If there were no such structures, then even when the signaling complex is formed, the diffusion rate of such a complex would be almost the same as that of the single receptor molecules, as diffusion theory teaches us (Saffman and Delbrück, 1975).

Therefore, in the plasma membrane, oligomerization or molecular complex formation is tied to immobilization by the membrane skeleton fence and anchored-protein pickets.

19.8 A Paradigm Shift of the Plasma Membrane Structure Concept is Necessary: From the Simple Two-dimensional Continuum Fluid Model to the Compartmentalized Fluid Model

As described above, the membrane-skeleton "fence" and the anchored-protein "picket" together solved the two long-standing problems of molecular diffusion in the plasma membrane: (1) the oligomerization-induced slowing of diffusion and (2) the reduced diffusion coefficients of membrane molecules in the plasma membrane, relative to those found in artificial membranes, by a factor of $\sim$ 20. These results could not be explained by the two-dimensional continuum fluid model. The two-dimensional continuum fluid model is just fine, as long as the spatial scale is limited to the size of the original cartoon depicted by Singer and Nicolson ([66], although at the smaller limit of the molecular scale, the continuum model would also fail), which is about 10 nm $\times$ 10 nm, based on the number of lipid molecules in the cartoon (Figure 19.3 inset). However, in spatial scales over several 10s of nm in the plasma membrane, simple-minded extensions of the fluid-mosaic model of Singer and Nicolson and the theory by Saffman–Delbrück fail. The cell seems to have developed (during evolution) means to control the long-range diffusion of membrane molecules and to make this control sensitive to the diffusant size. The long-range control of diffusion appears to be carried out by the actin-based membrane skeleton, as indicated by the partitioning (corralling) effect of the membrane skeleton and the rows of anchored-protein pickets.

Furthermore, when the cell needs to build a macroscopic diffusion barrier that blocks the diffusion of even phospholipids over the barrier region, like that found in the initial segment region of the neuronal cell membrane, the cell achieves this task by forming very dense picket-fences in the barrier region, effectively blocking the diffusion of membrane molecules across this region [19,39,80].

As such, a paradigm shift for the concept of plasma membrane structures in the space scales greater than 10 nm is required, from the two-dimensional continuum fluid to the compartmentalized fluid, in which its constituent molecules undergo hop diffusion over the compartments.

An important corollary of these results is that all of the diffusion coefficients obtained by FRAP, single-molecule techniques at slow rates (like a video rate), or fluorescence correlation spectroscopy (FCS) must be considered as "the *effective diffusion coefficients*", which may be useful only when the involved time-space window is specified [10, 12, 15, 38, 54, 55, 62, 67]. One should be clearly aware that membrane molecules do *not* undergo simple Brownian diffusion, although they may undergo *"effective simple Brownian diffusion" in limited time-space windows, generally in time scales longer than several 10s of milliseconds and in spatial scales greater than 0.3 μm.*

We emphasized the importance of tracking single molecules at enhanced frame rates. Thus far, the frame rate has been up to 40 000 frames per second (fps, 25 μs/frame) for single-particle tracking and 300 fps for single fluorescent-molecule tracking. The improvements have been continued in our laboratory, and currently, the frame rates are 250 000 fps (4 μs/frame) for single-particle tracking and 20 000 fps (50 μs/frame) for single fluorescent-molecule tracking. Since the rotational (reorientational) correlation times for monomeric proteins in the membrane (monomeric rhodopsin in reconstituted membranes, Kusumi and Hyde [21], Kusumi et al. [23] and for 40-nm colloidal gold particles in water are both about a few microseconds, further improvements in the frame rate would make the tracking too sensitive to rotational diffusion, and obscure the true displacement of molecules in space. Therefore, this time resolution of 4 μs is just about the useful limitation of the frame rate in studying molecular diffusion in the cell membrane using single-particle tracking. In the present article, we pay special attention to the short-range regulation mechanisms. However, the cell might also use some means for long-range regulations, perhaps combining the corralling and dragging effects of the cytoskeleton [24, 27]. For the detection of such long-range mechanisms, slower rate of observations would be required.

Acknowledgments

This research was supported in part by Health and Labour Sciences Research Grant nano-001 to N. Morone, and Grants-in-Aid for Scientific Research from the MEXT to N. Morone and A. Kusumi, and that on Priority Areas from the MEXT to A. Kusumi.

References

1 Borgdorff, A.J., and Choquet, D. *Nature* 2002, 417, 649–53.

2 Bussell, S.J., Hammer, D.A., and Koch, D.L. *J. Fluid Mech.* 1994, 258, 167–190.

3 Bussell, S.J., Koch, D.L., and Hammer, D.A. *Biophys. J.* 1995, 68, 1836–49.

4 Daumas, F., Destainville, N., Millot, C., Lopez, A., Dean, D., and Salome, L. *Biophys. J.* 2003a, 84, 356–66.

5 Daumas, F., Destainville, N., Millot, C., Lopez, A., Dean, D., and Salome, L. *Biochem. Soc. Trans.* 2003b, 31, 1001–5.

6 De Brabander, M., Geuens, G., Nuydens, R., Moeremans, M., and De Mey, J. *Cytobios.* 1985, 43, 273–83.

7 De Brabander, M., Nuydens, R., Geerts, H., and Hopkins, C.R. *Cell Motil. Cytoskelet.* 1988, 9, 30–47.

8 De Brabander, M., Nuydens, R., Ishihara, A., Holifield, B., Jacobson, K., and Geerts, H. *J. Cell Biol.* 1991, 112, 111–24.

9 Dietrich, C., Volovyk, Z.N., Levi, M., Thompson, N.L., and Jacobson, K. *Proc. Natl. Acad. Sci. U.S.A.* 2001, 98, 10642–7.

10 Feder, T.J., Brust-Mascher, I., Slattery, J.P., Baird, B., and Webb, W.W. *Biophys. J.* 1996, 70, 2767–73.

11 Frick, M., Schmidt, K., and Nichols, B.J. *Curr. Biol.* 2007, 17, 462–7.

12 Fujiwara, T., Ritchie, K., Murakoshi, H., Jacobson, K., and Kusumi, A. *J. Cell Biol.* 2002, 157, 1071–81.

13 Gambin, Y., Lopez-Esparza, R., Reffay, M., Sierecki, E., Gov, N.S., Genest, M., Hodges, R.S., and Urbach, W. *Proc. Natl. Acad. Sci. U.S.A.* 2006, 103, 2098–102.

14 Gelles, J., Schnapp, B.J., and Sheetz, M.P. *Nature* 1988, 331, 450–3.

15 Ghosh, R.N., and Webb, W.W. *Biophys. J.* 1994, 66, 1301–18.

16 Harms, G.S., Cognet, L., Lommerse, P.H., Blab, G.A., Kahr, H., Gamsjager, R., Spaink, H.P., Soldatov, N.M., Romanin, C., and Schmidt, T. *Biophys. J* 2001, 81, 2639–46.

17 Hegener, O., Prenner, L., Runkel, F., Baader, S.L., Kappler, J., and Haberlein, H. *Biochemistry* 2004, 43, 6190–9.

18 Iino, R., Koyama, I., and Kusumi, A. *Biophys. J.* 2001, 80, 2667–77.

19 Kobayashi, T., Storrie, B., Simons, K., and Dotti, C.G. *Nature* 1992, 359, 647–50.

20 Kucik, D.F., Elson, E.L., and Sheetz, M.P. *Nature* 1989, 340, 315–7.

21 Kusumi, A., and Hyde, J.S. *Biochemistry* 1982, 21, 5978–83.

22 Kusumi, A., Nakada, C., Ritchie, K., Murase, K., Suzuki, K., Murakoshi, H., Kasai, R.S., Kondo, J., and Fujiwara, T. *Annu. Rev. Biophys. Biomol. Struct.* 2005, 34, 351–78.

23 Kusumi, A., Sakaki, T., Yoshizawa, T., and Ohnishi, S. *J. Biochem. (Tokyo)* 1980, 88, 1103–11.

24 Kusumi, A., and Sako, Y. *Curr. Opin. Cell Biol.* 1996, 8, 566–74.

25 Kusumi, A., Sako, Y., and Yamamoto, M. *Biophys. J.* 1993, 65, 2021–40.

26 Kusumi, A., Subczynski, W.K., and Hyde, J.S. *Proc. Natl. Acad. Sci. U.S.A.* 1982, 79, 1854–58 .

27 Kusumi, A., Suzuki, K., and Koyasako, K. *Curr. Opin. Cell Biol.* 1999, 11, 582–90.

28 Lee, C.C., and Petersen, N.O. *Biophys. J.* 2003, 84, 1756–64.

29 Lee, G.M., Zhang, F., Ishihara, A., McNeil, C.L., and Jacobson, K.A. *J. Cell Biol.* 1993, 120, 25–35.

30 Lenne, P.F., Wawrezinieck, L., Conchonaud, F., Wurtz, O., Boned, A., Guo, X.J., Rigneault, H., He, H.T., and Marguet, D. *EMBO J.* 2006, 25, 3245–56.

31 Lindblom, G., Johansson, L.B., and Arvidson, G. *Biochemistry* 1981, 20, 2204–7.

32 Lommerse, P.H., Vastenhoud, K., Pirinen, N.J., Magee, A.I., Spaink, H.P., and Schmidt, T. *Biophys. J.* 2006, 91, 1090–7.

33 Martin, D. S., Forstner, M. B., and Käs, J. A. *Biophys. J.* 2002, 83, 2109–17.

34 Mashanov, G.I., Tacon, D., Peckham, M., and Molloy, J.E. *J. Biol. Chem.* 2004, 279, 15274–80.

35 Morone, N., Fujiwara, T., Murase, K., Kasai, R.S., Ike, H., Yuasa, S., Usukura, J., and Kusumi, A. *J. Cell Biol.* 2006, 174, 851–62.

36 Murakoshi, H., Iino, R., Kobayashi, T., Fujiwara, T., Ohshima, C., Yoshimura, A., and

Kusumi, A. *Proc. Natl. Acad. Sci. U.S.A.* 2004, 101, 7317–22.

37 Murase, K., Fujiwara, T., Umemura, Y., Suzuki, K., Iino, R., Yamashita, H., Saito, M., Murakoshi, H., Ritchie, K., and Kusumi, A. *Biophys. J.* 2004, 86, 4075–93.

38 Nagle, J.F. *Biophys. J.* 1992, 63, 366–70.

39 Nakada, C., Ritchie, K., Oba, Y., Nakamura, M., Hotta, Y., Iino, R., Kasai, R.S., Yamaguchi, K., Fujiwara, T., and Kusumi, A. *Nat. Cell Biol.* 2003, 5, 626–32.

40 Nelson, S., Horvat, R.D., Malvey, J., Roess, D.A., Barisas, B.G., and Clay, C.M. *Endocrinology* 1999, 140, 950–957.

41 Nishimura, S.Y., Vrljic, M., Klein, L.O., McConnell, H.M., and Moerner, W.E. *Biophys. J.* 2006, 90, 927–38.

42 Paller, M.S. *J. Membr. Biol.* 1994, 142, 127–35.

43 Peters, R., and Cherry, R.J. *Proc. Natl. Acad. Sci. U.S.A.* 1982, 79, 4317–21.

44 Powles, G.J., Mallett, M.J.D., Rickayzen, G., and Evans, W.A.B. *Proc. R. Soc. Lond. A* 1992, 436, 391–403.

45 Qian, H., Sheetz, M.P., and Elson, E.L. *Biophys J* 1991, 60, 910–21.

46 Rothberg, K.G., Heuser, J.E., Donzell, W.C., Ying, Y.S., Glenney, J.R., and Anderson, R.G. *Cell* 1992, 68, 673–82.

47 Saffman, P.G. and Delbrück, M. *Proc. Natl. Acad. Sci. USA* 1975, 72, 3111–3.

48 Sako, Y., and Kusumi, A. *J. Cell Biol.* 1994, 125, 1251–64.

49 Sako, Y., and Kusumi, A. *J. Cell Biol.* 1995, 129, 1559–74.

50 Sako, Y., Minoghchi, S., and Yanagida, T. *Nat. Cell Biol.* 2000, 2, 168–72.

51 Sako, Y., Nagafuchi, A., Tsukita, S., Takeichi, M., and Kusumi, A. *J. Cell Biol.* 1998, 140, 1227–40.

52 Saxton, M.J. *Biophys. J.* 1989, 55, 21–8.

53 Saxton, M.J. *Biophys. J.* 1990, 57, 1167–77.

54 Saxton, M.J. *Biophys. J.* 1994, 67, 2110–9.

55 Saxton, M.J. *Biophys. J.* 1996, 70, 1250–62.

56 Saxton, M.J. *Biophys. J.* 1997, 72, 1744–53..

57 Saxton, M.J., and Jacobson, K. *Annu. Rev. Biophys. Biomol. Struct.* 1997, 26, 373–99.

58 Schmidt, K., and Nichols, B.J. *Curr. Biol.* 2004, 14, 1002–6.

59 Schmidt, T., Schutz, G.J., Baumgartner, W., Gruber, H.J., and Schindler, H. *J. Phys. Chem.* 1995, 99, 17662–17668.

60 Schnapp, B.J., Gelles, J., and Sheetz, M.P. *Cell Motil. Cytoskelet.* 1988, 10, 47–53.

61 Schutz, G.J., Kada, G., Pastushenko, V.P., and Schindler, H. *EMBO J.* 2000, 19, 892–901.

62 Sheets, E.D., Lee, G.M., Simson, R., and Jacobson, K. *Biochemistry* 1997, 36, 12449–58.

63 Sheetz, M.P. *Semin. Hematol.* 1983, 20, 175–188.

64 Sheetz, M.P., Schindler, M., and Koppel, D.E. *Nature* 1980, 285, 510–1.

65 Sheetz, M.P., Turney, S., Qian, H., and Elson, E.L. *Nature* 1989, 340, 284–8.

66 Singer, S.J., and Nicolson, G.L. *Science* 1972, 175, 720–31.

67 Suzuki, K., Ritchie, K., Kajikawa, E., Fujiwara, T., and Kusumi, A. *Biophys. J.* 2005, 88, 3659–80.

68 Suzuki, K.G., Fujiwara, T.K., Edidin, M., and Kusumi, A. *J. Cell Biol.* 2007a, 177, 731–42.

69 Suzuki, K.G., Fujiwara, T.K., Sanematsu, F., Iino, R., Edidin, M., and Kusumi, A. *J. Cell Biol.* 2007b, 177, 717–30.

70 Takeuchi, M., Miyamoto, H., Sako, Y., Komizu, H., and Kusumi, A. *Biophys. J.* 1998, 74, 2171–83.

71 Tank, D.W., Wu, E.S., and Webb, W.W. *J. Cell Biol.* 1982, 92, 207–12.

72 Tomishige, M., Sako, Y., and Kusumi, A. *J. Cell Biol.* 1998, 142, 989–1000.

73 Tsuji, A., Kawasaki, K., Ohnishi, S., Merkle, H., and Kusumi, A. *Biochemistry* 1988, 27, 7447–52.

74 Tsuji, A., and Ohnishi, S. *Biochemistry* 1986, 25, 6133–9.

75 Vaz, W.L., Criado, M., Madeira, V.M., Schoellmann, G., and Jovin, T.M. *Biochemistry* 1982, 21, 5608–12.

76 Vaz, W.L., Goodsaid-Zalduondo, F., and Jacobson, K. *FEBS Lett.* 1984, 174, 199–207.

77 Vrljic, M., Nishimura, S.Y., Brasselet, S., Moerner, W.E., and McConnell, H.M. *Biophys. J.* 2002, 83, 2681–92.

78 Wenger, J., Conchonaud, F., Dintinger, J., Wawrezinieck, L., Ebbesen, T.W., Rigneault,

H., Marguet, D., and Lenne, P.F. *Biophys. J.* 2007, 92, 913–9.

79 Wieser, S., Moertelmaier, M., Fuertbauer, E., Stockinger, H., and Schutz, G.J. *Biophys. J.* 2007, 92, 3719–28.

80 Winckler, B., Forscher, P., and Mellman, I. *Nature* 1999, 397, 698–701.

81 Wu, E.S., Tank, D.W., and Webb, W.W. *Proc. Natl. Acad. Sci. USA* 1982, 79, 4962–6.

SERIES

ナロンド・バイオイメージング

第3回

蛍光プローブ開発秘話：Pericam

Anecdote of fluorescent probe development : Pericam

永井健治

Ⅰ．研究事始め

1．卒業研究のころ

筆者が蛍光プローブの開発をはじめたきっかけを説明するには，1991年の筑波大学での卒業研究までさかのぼらなければならない．散逸構造論や反応拡散理論を（ちょっと）かじってプリゴジーンやチューリングなどにすっかり傾倒していた筆者は，卒業研究をするならその生物学への展開がおもしろいだろうと考えた．そして，レニン-アンジオテンシン系の研究で有名な村上和雄博士（筑波大学名誉教授）の研究室にて講師をされていた上野直人博士（現 基礎生物学研究所 教授）の指導のもと，“アフリカツメガエルにおける中胚葉誘導の分子生物学的解析”を卒業研究に選んだ．分泌蛋白質アクチビンが濃度依存的に異なる中胚葉組織パターンを誘導する現象は，まさにうってつけの題材だったからである．

ところが，研究を開始して3カ月もしないうち，自分自身の研究に疑問をもつようになった．結局，筆者のやっていることは“遺伝子の過剰発現や欠損などの摂動をあたえて，表現型やほかの遺伝子発現がどうなるかを確認し，その遺伝子の役割を確定する”だけじゃないかと．もちろん重要な研究だけれども，それではある生理現象の原因と結果を調べているだけで，その途中でなにが起こっているのかはブラックボックスのまま．まさに，痒い背中に手が届かない感じである．チューリングの反応拡散論的な観点でパターン形成を理解するには，静的な（死んだ）試料を解析していてはだめで，アクチビンのような中胚葉誘導因子がどのように分泌されて濃度勾配を形成していくのかを，生きたアフリカツメガエル胚のなかでとらえていくことがなによりも肝要である．さらに，中胚葉誘導因子の濃度情報が細胞内でどのようにデコードされていくのかも，シグナル伝達にかかわる蛋白質がつくりだすネットワークの機能を可視化することで理解する必要がある．

当時の解析技術ではできっこないことを，研究室の同級生や先輩に声を大にして語っていたのが，昨日のことのように思い出される．青二才が偉そうなことをぬかしていたので，研究室の助手が，毎日，眉間に皺を寄せていたのはいうまでもない．“永井，おまえは偉そうな口を叩くまえに言われたことをやれ”とか“おまえが考えることくらいすでに誰かが考えてやっているんだよ”と，よく説教されたものである．事実，すでにこのとき，近藤 滋博士（現 名古屋大学 教授）が，チューリングの反応拡散理論で熱帯魚の皮膚模様を説明する研究を展開しつつあった．

2．X線顕微鏡法との出会い

そんな折，筑波大学物理工学系の青木貞雄博士がX線顕微鏡の開発を行なっていると，上野博士が紹介してくれた．可視光よりも波長がはるかに短いX線を用いれば，理論上は生きた個体のなかの現象を分子レベルの空間分解能で観ることができるのではないか？　と胸を躍らせ，上野博士に懇願して青木研への学内留学を許可してもらった．卒業研究から一転，修士課程では，青木研自作の拡大投影型X線マイクロ（下やウォルターミラー型X線顕微鏡などの機

Takeharu Nagai
北海道大学電子科学研究所 ナノシステム生理学研究分野
E-mail：tnagai@es.hokudai.ac.jp
URL：http://nano.es.hokudai.ac.jp/